Environmental Research Letters

LETTER • **OPEN ACCESS**

Multi-model ensemble projections of European river floods and high flows at 1.5, 2, and 3 degrees global warming

To cite this article: Stephan Thober *et al* 2018 *Environ. Res. Lett.* **13** 014003

Environmental Research Letters

CrossMark

OPEN ACCESS

RECEIVED
7 July 2017

REVISED
31 October 2017

ACCEPTED FOR PUBLICATION
29 November 2017

PUBLISHED
3 January 2018

LETTER

Multi-model ensemble projections of European river floods and high flows at 1.5, 2, and 3 degrees global warming

Stephan Thober[1,6], Rohini Kumar[1], Niko Wanders[2,3], Andreas Marx[1], Ming Pan[3], Oldrich Rakovec[1,4], Luis Samaniego[1], Justin Sheffield[5], Eric F Wood[3] and Matthias Zink[1]

[1] Department of Computational Hydrosystems, Helmholtz Centre for Environmental Research - UFZ, Leipzig, Germany
[2] Department of Physical Geography, Faculty of Geosciences, University Utrecht, The Netherlands
[3] Department of Civil and Environmental Engineering, Princeton University, Princeton, NJ, United States of America
[4] Czech University of Life Sciences, Faculty of Environmental Sciences, Prague, 169 00, Czech Republic
[5] Geography and Environment, University of Southampton, Southampton, United Kingdom
[6] Author to whom any correspondence should be addressed.

E-mail: stephan.thober@ufz.de

Keywords: climate change, 1.5 degree global warming, mHM, Noah-MP, PCR-GLOBWB, Europe, floods

Supplementary material for this article is available online

Abstract

Severe river floods often result in huge economic losses and fatalities. Since 1980, almost 1500 such events have been reported in Europe. This study investigates climate change impacts on European floods under 1.5, 2, and 3 K global warming. The impacts are assessed employing a multi-model ensemble containing three hydrologic models (HMs: mHM, Noah-MP, PCR-GLOBWB) forced by five CMIP5 general circulation models (GCMs) under three Representative Concentration Pathways (RCPs 2.6, 6.0, and 8.5). This multi-model ensemble is unprecedented with respect to the combination of its size (45 realisations) and its spatial resolution, which is 5 km over the entirety of Europe. Climate change impacts are quantified for high flows and flood events, represented by 10% exceedance probability and annual maxima of daily streamflow, respectively. The multi-model ensemble points to the Mediterranean region as a hotspot of changes with significant decrements in high flows from −11% at 1.5 K up to −30% at 3 K global warming mainly resulting from reduced precipitation. Small changes ($< \pm 10\%$) are observed for river basins in Central Europe and the British Isles under different levels of warming. Projected higher annual precipitation increases high flows in Scandinavia, but reduced snow melt equivalent decreases flood events in this region. Neglecting uncertainties originating from internal climate variability, downscaling technique, and hydrologic model parameters, the contribution by the GCMs to the overall uncertainties of the ensemble is in general higher than that by the HMs. The latter, however, have a substantial share in the Mediterranean and Scandinavia. Adaptation measures for limiting the impacts of global warming could be similar under 1.5 K and 2 K global warming, but have to account for significantly higher changes under 3 K global warming.

1. Introduction

Floods are a major natural hazard to societies, threatening lives and livelihoods, as well as infrastructure. During the period 1950–2015, these events affected around 18 million people and caused economic losses of approximately 133 billion USD in Europe (Guha-Sapir *et al* 2017). By the end of the 21st century, climate change is projected to alter European floods in complex ways. Decreases in flood peaks are reported for Northern Europe in Andréasson *et al* (2004), Arheimer and Lindstrom (2015), Alfieri *et al* (2015), Roudier *et al* (2016) and Donnelly *et al* (2017). These reductions are caused by increased temperatures that reduce snow accumulation in winter leading to less melting water in spring. Strong decreases in annual precipitation in the

Mediterranean (Rajczak *et al* 2013, Alfieri *et al* 2015) also diminish the magnitude of floods in this region (Rojas *et al* 2012, Alfieri *et al* 2015). Different signs of change are in general reported for Central Europe and the British Isles (Kay and Jones 2012, Alfieri *et al* 2015). A comprehensive review on the mechanisms causing flood changes in Europe including climate change can be found in Hall *et al* (2014). These studies typically employ Representative Concentration Pathway (RCP) scenarios which cover a range of global warming from 0.3–1.7 K under RCP2.6 to 2.6–4.1 K under RCP8.5 (Collins *et al* 2013, James *et al* 2017). No explicit analysis is carried out for projections of floods at different warming levels (e.g. 2 and 3 K).

The 2015 Paris agreement on climate change included the ambitious goal to 'pursue efforts to limit the temperature increase to 1.5 °C' (UNFCC 2015). Currently, the number of studies that explicitly investigate the impact of different degrees of warming (i.e. 1.5, 2, and 3 K) on floods at the pan-European scale is limited. Gosling *et al* (2016) reported contrasting results for the Central European Rhine and the Mediterranean Tagus River. Small positive and negative changes in high flows (Q5) of less than 10% were reported for the Rhine under 1, 2, and 3 K global warming, whereas strong decreases up to −30% under 3 K global warming were projected for the Tagus. Recently, Donnelly *et al* (2017) reported higher impacts of climate change on median annual maximum runoff with increasing global temperatures (1.5, 2, and 3 K). Their projected increases in the Mediterranean disagree with Rojas *et al* (2012), Alfieri *et al* (2015), and Gosling *et al* (2016) that estimated decreases in floods. These differences may be explained by the employed bias correction of the climate model data, i.e. trend-preserving bias correction in Gosling *et al* (2016) versus quantile-mapping in Donnelly *et al* (2017). An European assessment of changes in floods for different warming levels using consistent trend-preserving bias corrected dataset has, however, not been conducted so far.

Uncertainty is omnipresent within studies of climate change impacts on floods. The choice of general circulation model (GCM), downscaling procedure, and hydrological model (HM) contribute substantially to the total uncertainty (Bosshard *et al* 2014). Internal climate variability originating from different initial states of GCM simulations has also been recognised as a source of uncertainty (Deser *et al* 2014). Hydrologic models were identified as an uncertainty factor that cannot be neglected in Dankers *et al* (2014), Gosling *et al* (2016) and Donnelly *et al* (2017), including the estimation of hydrologic model parameter (Wilby 2005). An European uncertainty assessment at a high resolution (5 km) has so far only quantified the contribution by different GCMs (Alfieri *et al* 2015).

In this study, a comprehensive impact and uncertainty assessment is conducted for European high flows (Q_{10}) and flood events (Q_{max}) at a high 5 km spatial resolution under 1.5, 2, and 3 K global warming. A consistent multi-model ensemble with 45 members (5 GCMs, 3 RCPs, 3 HMs) is employed. The research questions are as follows:

1. What is the magnitude and significance of change in high flows and floods in Europe under 1.5, 2, and 3 K global warming?
2. How significant are the projected changes of high flows and floods between the three global warming levels?
3. How much do the GCMs and HMs contribute to the overall uncertainty for the particular warming levels?

2. Methods

2.1. General circulation models and differential warming periods

Temperature and precipitation from five GCMs (HadGEM2-ES, IPSL-CM5A-LR, MIROC-ESM-CHEM, GFDL-ESM2M and NorESM1-M) is used to force three HMs at the daily time scale for the period 1950–2099 under three RCPs (2.6, 6.0, and 8.5), which was made available by the ISI-MIP project (Warszawski *et al* 2014, Hempel *et al* 2013a). These models have also been widely used for impact studies (Krysanova and Hattermann 2017). This GCM data were downscaled and bias-corrected at a 0.5° global resolution using a trend-preserving approach (Hempel *et al* 2013b). The 0.5° data is further interpolated within the EDgE project (edge.climate.copernicus.eu) to a 5 km grid over Europe using external drift kriging, which enables HM application at high spatial resolution (Wood *et al* 2011, Bierkens *et al* 2015). One variogram for each meteorological variable (i.e. precipitation and temperature) is used for the interpolation, which is derived from daily E-OBS station data (Haylock *et al* 2008). This approach does not modify long-term trends and is suitable for climate change impact studies.

The period 1971–2000 is selected to represent present-day conditions (1980s in the following) because 1991–2000 is the last decade fully within the historical period of the GCM data. This period is estimated to correspond to a global warming of 0.46 K to pre-industrial conditions in 1881–1910 (Vautard *et al* 2014). Global warming periods of 30 years for 1.5, 2, and 3 K are estimated with respect to the 1980s employing a time sampling approach (James *et al* 2017, see supplementary material section S1, available at stacks.iop.org/ERL/13/014003/mmedia). Global warming since preindustrial conditions might be about 0.11 K higher than the 0.46 K assumed here (Hawkins *et al* 2017), which results in warming periods starting about 2–6 years earlier (not shown). This only has a minor impact on the results because 30 year median values are used in the analysis.

2.2. Hydrologic models

Runoff is simulated by three HMs (mHM, Noah-MP, and PCR-GLOBWB) and routed through the same 5 km river network using the multi-scale routing model that has been developed originally for mHM (Samaniego *et al* 2010). All models were setup using the same morphologic, land cover, and soil data such that differences among models only originate from different process representations. The mesoscale hydrological model (mHM, www.ufz.de/mhm) is a process-based HM that has been developed for scales from 1 km–50 km (Samaniego *et al* 2010, Kumar *et al* 2013). PCR-GLOBWB was developed to represent the terrestrial water cycle, including the human water management, at the global and continental scale with a special emphasis on the groundwater component (van Beek *et al* 2011, Wanders and Wada 2015). Noah-MP is the land surface component of the Weather Research and Forecast Model representing both the terrestrial water and energy cycle (Niu *et al* 2011). These three models comprise a wide range of process representations from different conceptualisations of runoff delay using non-linear reservoirs (mHM and PCR-GLOBWB) to numerically computing the Richards equation (Noah-MP). The latter is a physically-based representation for the movement of water in unsaturated soils (Chow *et al* 1988). Model parameters are calibrated using the E-OBS meteorologic data (Haylock *et al* 2008) at nine distinct catchments located in Spain, UK, and Norway. Automatic calibration is employed for mHM (following Rakovec *et al* 2016) and PCR-GLOBWB. Noah-MP is calibrated manually adjusting the parameter for surface evaporation resistance based on the analysis by Cuntz *et al* (2016).

Using the GCM forcing, all models show a reasonable reproduction of observed indicators at 165 gauging stations (see supplementary section S2). The observed flood indicator is on average underestimated by the multimodel mean by 10% with a standard deviation of 38%. The simulation results for the high flow indicator show a relatively higher bias of 44% for the multimodel mean with a standard deviation of 47%. This is a very rigorous comparison because the high flow and flood indicators obtained from GCM-driven model simulations are directly compared against observations. As a result, higher biases then comparisons using observation-driven HM simulations can be expected. Notably, reducing HM bias through explicit parameter calibration may not reduce the HM uncertainty (e.g. intermodel difference; Mendoza *et al* 2015).

2.3. High flow and flood indicator

Two indicators of extreme streamflows are used in this study. These have been co-designed in close collaboration with stakeholders in the water sector across Europe within the EDgE project. The indicators are:

- High flows: the streamflow exceeded 10% of the time (Q_{10}).
- Floods: the annual maximum streamflow (Q_{max}).

Both indicators are estimated for each year within a given 30 year period. The median of these 30 year values is then considered for the evaluation, which is regarded as a robust estimator for a flow duration curve (Vogel and Fennessey 1994, Blum *et al* 2017). Furthermore, only river basins with a contributing area larger than 1000 km^2 are considered in this study to limit the errors due to incorrect delineation of small tributaries and headwater river basins in the routing process.

2.4. Evaluation metrics, significance test and uncertainty contribution

The impact of climate change is quantified for a given indicator by calculating the relative change between a future 30 year median and the median of the 1980s (1971–2000). The non-parametric Wilcoxon rank-sum test is applied to the two 30 year samples to test the null hypothesis of equal medians, which is frequently used in climate impact studies (Gosling *et al* 2016). Finally, the percentage of ensemble members indicating a significant difference at a 5% significance level is quantified to assess the robustness of ensemble projections. The results are aggregated to the IPCC AR5 European regions (Kovats *et al* 2011) based on the stratification presented in Metzger *et al* (2005) (see supplementary section S3).

The signal to noise ratio is used to quantify the uncertainty of projected changes (Hall *et al* 2014, Giuntoli *et al* 2015). The signal is estimated as the ensemble median and the noise as the inter-quartile range of the multimodel ensemble, i.e. the difference between the 25th and the 75th percentile of the ensemble members. The sequential sampling approach by Samaniego *et al* (2017) is used here to quantify the individual contributions by GCMs and HMs (see supplementary section S4).

3. Results and discussion

3.1. Relative changes for 1.5, 2, and 3 K global warming

The magnitude of projected changes for high flows (figures 1(*a*)–(*c*)) and floods (figures 1(*g*)–(*i*)) amplify with enhanced global warming from 1.5 K–3 K. Strong increases in high flows up to 12% are projected in the Northern region under 3 K global warming (table 1). Conversely, large decreases are projected in the Mediterranean. These are of the order of −10% on average for a 1.5 K global warming and further decrease to −30% for 3 K global warming. Particular hotspots of projected changes in the Mediterranean region are the Iberian Peninsula and the Balkans. The Atlantic and Continental regions can be considered as a transition zone between decreases in Southern and

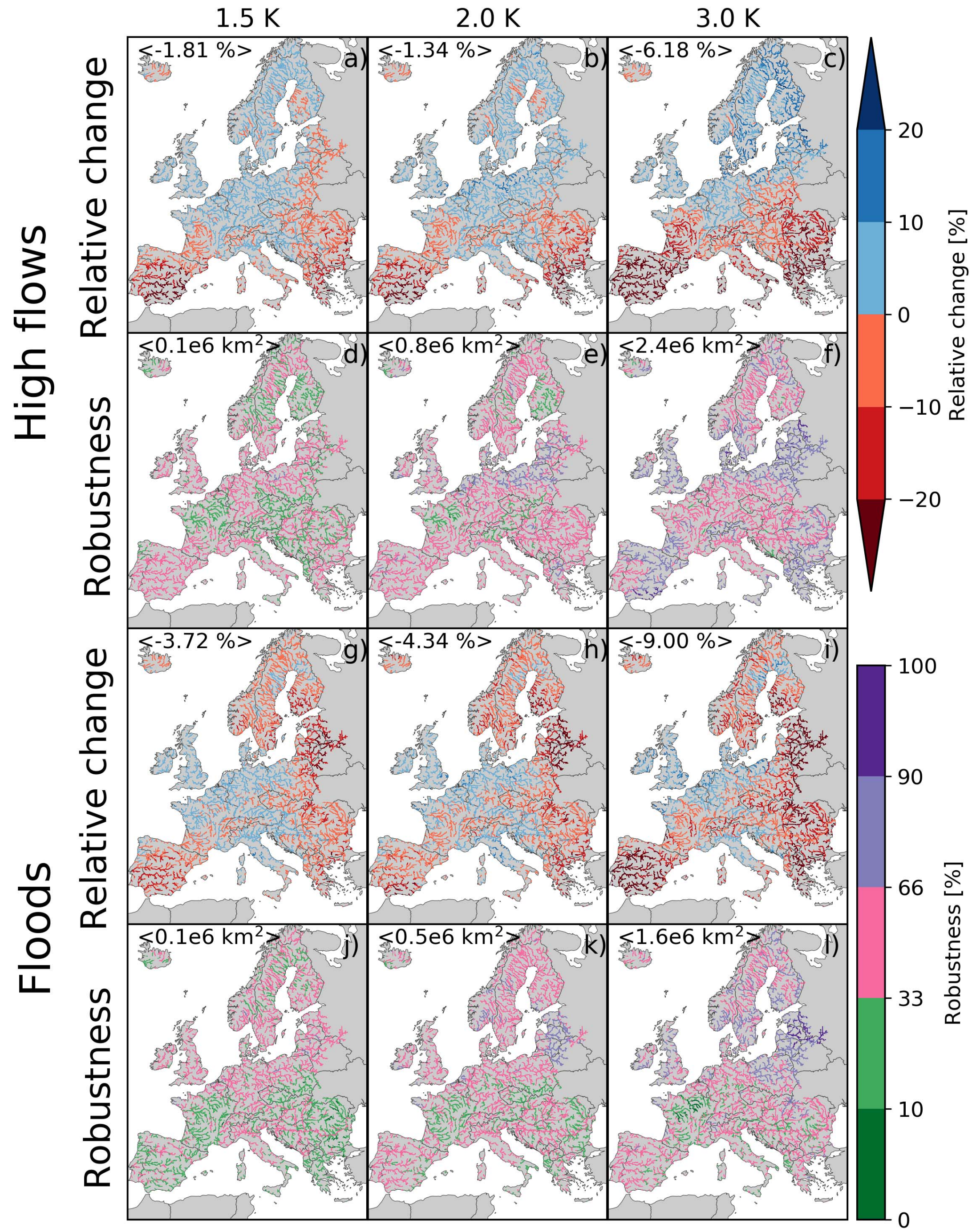

Figure 1. Relative changes of multi-model ensemble median for different warming levels in comparison to the reference period 1971–2000. Changes for high flows (Q_{10}) are shown in panels (*a*)–(*c*) and for floods (annual daily maximum) in panels (*g*)–(*i*) under increasing levels of global warming (columns from left to right: 1.5, 2, and 3 K). Percentage of ensemble members indicating robust changes for high flow and flood indicator in panels (*d*)–(*f*) and panels (*j*)–(*l*), respectively. The percentages follow the IPCC nomenclature of very unlikely ($< 10\%$), unlikely ($10\% < 33\%$), as likely as not ($33\% < 66\%$), likely ($66\% < 90\%$) and very likely ($> 90\%$). For high flows, the numbers given in $< \cdot >$ denote the spatial average. For floods, the numbers denote the total area (10^6 km^2) exhibiting at least likely changes. The total area of the study domain is 5.4×10^6 km^2.

increases in Northern Europe. Projected changes in these regions are generally less than 10% in magnitude (table 1).

On average, projected changes in floods are small (i.e. less than 10% in magnitude) with similar spatial patterns to high flows for all warming levels (figures 1(*g*)–(*i*)). It is worth noting that a relatively small change of 15% in annual maximum may lead to substantial changes in flood return periods with strong effects on adaptation planning (Hattermann *et al* 2016). As for high flows, the strongest decreases of floods are seen in the Mediterranean. The magnitude of changes is, however, reduced to −17% under 3 K global warming. A contrasting pattern to high flows is seen in the Northern region, where floods decrease by up to −5% under 3 K global warming and high flows

Table 1. Projected changes for high flow and flood indicator under different levels of warming stratified for IPCC regions (Kovats *et al* 2011) in per cent. The location of the IPCC regions is shown in the figure S4.

Warming level	Alpine	Atlantic	European regions Continental	Northern	Mediterranean
High flows					
1.5 K	1.8	2.8	−1.2	1.3	−10.6
2 K	1.4	3.1	−0.7	4.7	−12.7
3 K	1.3	−1.4	−8.9	11.9	−30.6
Floods					
1.5 K	−3.5	2.4	−2.5	−6.7	−4.8
2 K	−5.9	2.9	−2.2	−6.2	−4.7
3 K	−9.1	1.3	−8.7	−5.0	−16.9

increase up to 12%. This highlights the importance of considering multiple indicators that are relevant for different stakeholders. A decrease of floods in this region has been observed in several studies (Arheimer and Lindstrom 2015, Alfieri *et al* 2015, Roudier *et al* 2016). Increased temperature in snow dominated regions will alter snow dynamics, in particular decreases in snow pack are projected (Roudier *et al* 2016, Donnelly *et al* 2017) that will lead to less spring melt and consequently reduce spring floods. In the past decades, earlier snowmelt lead to a shift in timing of floods in this region (Bloeschl *et al* 2017).

The percentage of ensemble members projecting a robust change exhibits a substantial spatial variability for both indicators and all warming levels (figures 1(*d*)–(*f*) for high flows and figures 1(*j*)–(*l*) for floods). The area of likely changes increases with higher warming levels for both indicators. It is generally higher for high flows than for floods covering up to 2.4 and 1.6×10^6 km^2, respectively (total area of the study domain is 5.4×10^6 km^2). Likely changes are found mainly in regions with strong change signals. A large agreement among models is observed in the Baltic states for both high flows and floods, particularly at 3 K warming. Substantial disagreements are found in the Mediterranean under 3 K global warming, with changes in high flows being significant for more than 66% (likely change) of the ensemble members whereas this number reduces to less than 33% (unlikely) for floods.

Recently, Donnelly *et al* (2017) reported a stronger increase of high flows with increasing global warming. The herein projected magnitude and direction of changes are substantially different, particularly in the Mediterranean. It is worth noting that the indicators are estimated here for routed streamflow, whereas Donnelly *et al* (2017) used grid-specific runoff in their analysis. The streamflow of a particular river reach is the result of the grid-specific runoff routed over the entire upstream area, which is more relevant for flood conditions. Notably, the projected changes presented here are confirming those reported by Gosling *et al* (2016) for the Tagus River who used the same GCM forcing dataset. They are also in line with Alfieri *et al* (2015) and Rojas *et al* (2012) who estimated decreases in annual maximum streamflow of −30% by the end of the 21st century on the Iberian Peninsula.

To a large extent, the projected changes in the high flow indicator are related to the changes in annual total catchment precipitation (figures 2(*a*)–(*c*)), as highlighted by a coefficient of determination (r^2) larger than 0.5 for all warming levels. Higher r^2 values are observed for higher warming levels mostly because of the increased spread. There is, however, a considerable difference between positive and negative precipitation changes. Areas exhibiting a decrease in annual total precipitation are located mostly in the Mediterranean, Continental, and Atlantic regions and show higher r^2 than areas with positive precipitation changes. Annual precipitation is projected to increase mostly in the Northern region (see van Vliet *et al* 2015, for the same GCMs). An increase in this region has also been reported in other studies (Arheimer and Lindstrom 2015, Alfieri *et al* 2015, Donnelly *et al* 2017). In northern regions, high temperatures have a strong impact on snow processes with altered snow accumulation and melting. Snow acts as a buffer that diminishes the relationship between precipitation and high flows resulting in lower r^2 values compared to areas without a significant snow cover. In contrast, the flood indicator shows a weak correspondence to the changes in annual precipitation (figures 2(*d*)–(*f*)) regardless of the region and warming level. Other precipitation statistics, such as maximum five-day precipitation (*rx5day*) often used as an explanatory variable for changes in floods (Rojas *et al* 2012), do not exhibit a strong relationship either (figures 2(*g*)–(*i*)). One reason might be that GCMs are underestimating extreme precipitation amounts, in particular convective precipitation (Jacob *et al* 2014). However, recent research using an observation-based datasets indicates that a link between extreme precipitation and extreme streamflow is only found in few cases (Wasko and Sharma 2017). This highlights the complexity of flood events that not only depend on the total amount of precipitation but also on its spatial distribution, time evolution, and antecedent soil moisture conditions (Bloeschl *et al* 2013). It is worth noting that changes in *rx5day* are mostly positive regardless of the warming level, which has also been reported in the literature for end of the century projections (Rojas *et al* 2012, Alfieri *et al* 2015). To some extent, the Atlantic and Mediterranean regions show higher sensitivity to changes in *rx5day*, which might be related to the minor

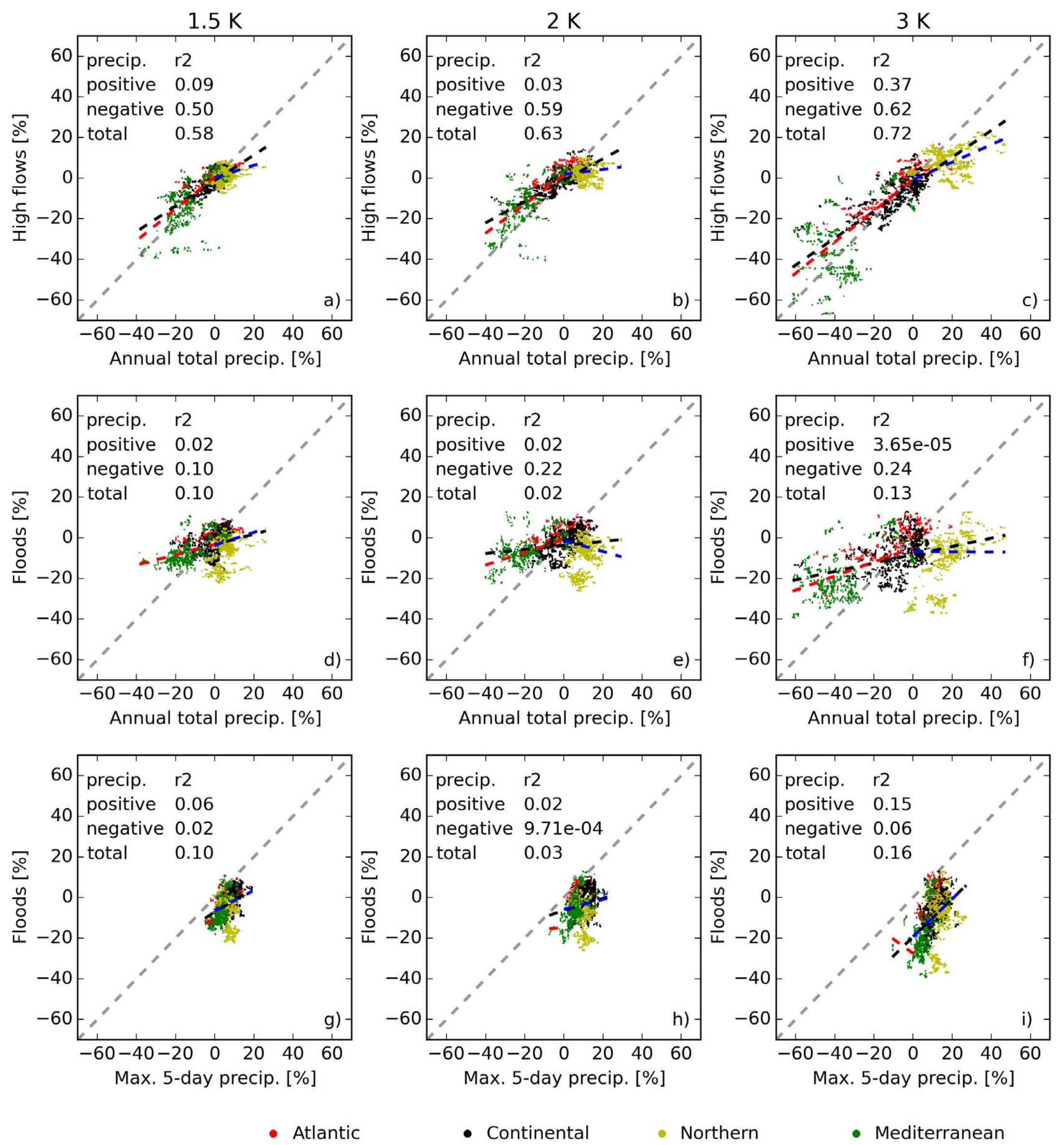

Figure 2. Panels (*a*)–(*c*): Scatter plot between projected relative change of multi-model ensemble median for high flows and annual total precipitation for different levels of warming (columns from left to right: 1.5, 2, and 3 K). Panels (*d*)–(*f*): same as panels (*a*)–(*c*), but for floods. Panels (*g*)–(*i*): Scatter plot between projected relative change for floods and maximum five-day precipitation (rx5day) for different levels of warming. In each panel, the coefficient of determination is given for data points exhibiting positive precipitation change, negative precipitation change, and all points. Data points are coloured according to the region they belong to (Alpine region not shown because of limited sample size). Dashed line show the fit of a linear regression (red—negative precipitation, blue—positive precipitation, black—total precipitation).

importance of snow processes in these regions (table S4: r^2 values for individual regions). While our analysis indicates that precipitation-based extreme indicators (*rx5day*) may not be suitable for analysing floods, future research should examine this relationship in greater detail.

3.2. Differences in high flow and floods between 1.5, 2, and 3 K

A particular focus of this study is to evaluate changes in high flow and flood indicators between 1.5, 2 and 3 K global warming. As expected, larger differences in global temperatures lead to larger differences in high flow and flood indicators across Europe and for all stratified regions (figure 3). The differences in the magnitude of relative change is less than 10% for both indicators between a 1.5 K and 2 K warmer world with robust signals found in at most 8% of the ensemble members because of the large uncertainties of the relative changes at both the 1.5 K and 2 K global warming and the relatively small change in global mean temperatures. Across all regions, higher and more robust changes are observed between all other warming levels.

The impact of climate change does not only depend on the incremental level of warming, but also on the absolute value of global mean temperatures. This can be seen by comparing distributions of relative change when moving from present-day climate (1980s) to a 1.5 K warming and from a 2 K to a 3 K warming.

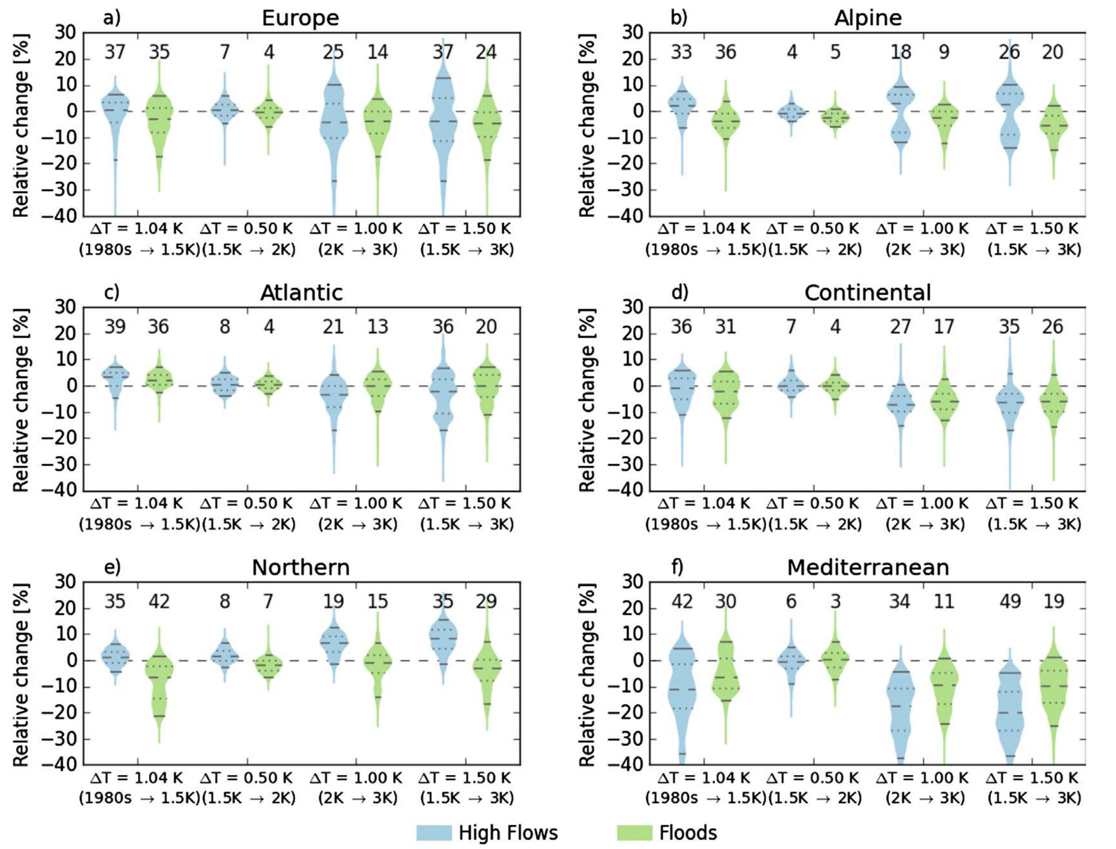

Figure 3. Distribution of relative changes for the multi-model ensemble median between different warming levels. Panels give average information over the IPCC Europe regions presented in Kovats *et al* (2011) (see figure S4). Blue violins display the distribution of projected changes for the high flow indicator and green ones for floods. For each violin, the solid line displays the 5th and 95th percentile, dotted lines the 25th and 75th percentile, and the dashed line the median. Numbers on top of the violins denote the robustness, i.e. percentage of ensemble members with a p-value less than 0.05 in the Wilcoxon rank sum test.

In both cases, the increase of global temperature is in a similar order (about 1 K), but the distribution of differences varies across regions. This is most evident for the Alpine region (figure 3(*b*)). Projected high flow changes exhibit a bimodal distribution moving from 2 K to 3 K global warming, but a unimodal one from the 1980s to 1.5 K warming. The bimodal distribution is due to a different response in the Alps and the Alpine regions in Norway (see supplementary section S6). Higher temperatures lead to a shorter snow season in both of these mountainous regions, but precipitation is projected only to increase in Norway.

Across all regions, the robustness of projected changes is higher between the 1980s and a 1.5 K warming than between a 2 K and 3 K warming (figure 3). In the former, 35%–37% of the ensemble realisations indicate significant changes whereas these are only 14%–25% in the latter (figure 3(*a*)). This implies that the robustness depends on the absolute global warming level. Moreover, it is not distributed evenly over the continent. For high flows, regions exhibiting changes that are as likely as not (percentage from 33%–66%) are located in the Mediterranean and large parts of Eastern Europe (see figure S5). The differences in the relative changes for both indicators between 1.5 and 3 K global warming and their significance follow the same distributions as those between 2 and 3 K, but are more strongly pronounced because of the larger difference in global mean temperature. The significance is, however, in general smaller than between the 1980s and 1.5 K warming. One reason may be that the inter-annual variability within the 30 year samples is smaller for the 1980s than for the future periods. The variability is pathway dependent in the latter case. For example, a GCM with a global warming of 1.5 K might give a different response for a 30 year period with a strong temperature increase (e.g. under RCP 8.5) compared to a period with a nearly constant warming of 1.5 K (e.g. under RCP 2.6; see also figure S1). This is a limitation of the time sampling approach used here (James *et al* 2017).

Overall, this analysis highlights that the effort to limit global warming to 1.5 K (UNFCC 2015) would yield a limited benefit for high flow and flood indicators across Europe in comparison to 2 K global warming. The underlying uncertainty in the ensemble members precludes a robust distinction between changes under 1.5 K and 2 K. However, under a 1.5 K global warming, the projected changes are robust for at least 30% of the ensemble members in all stratified European regions

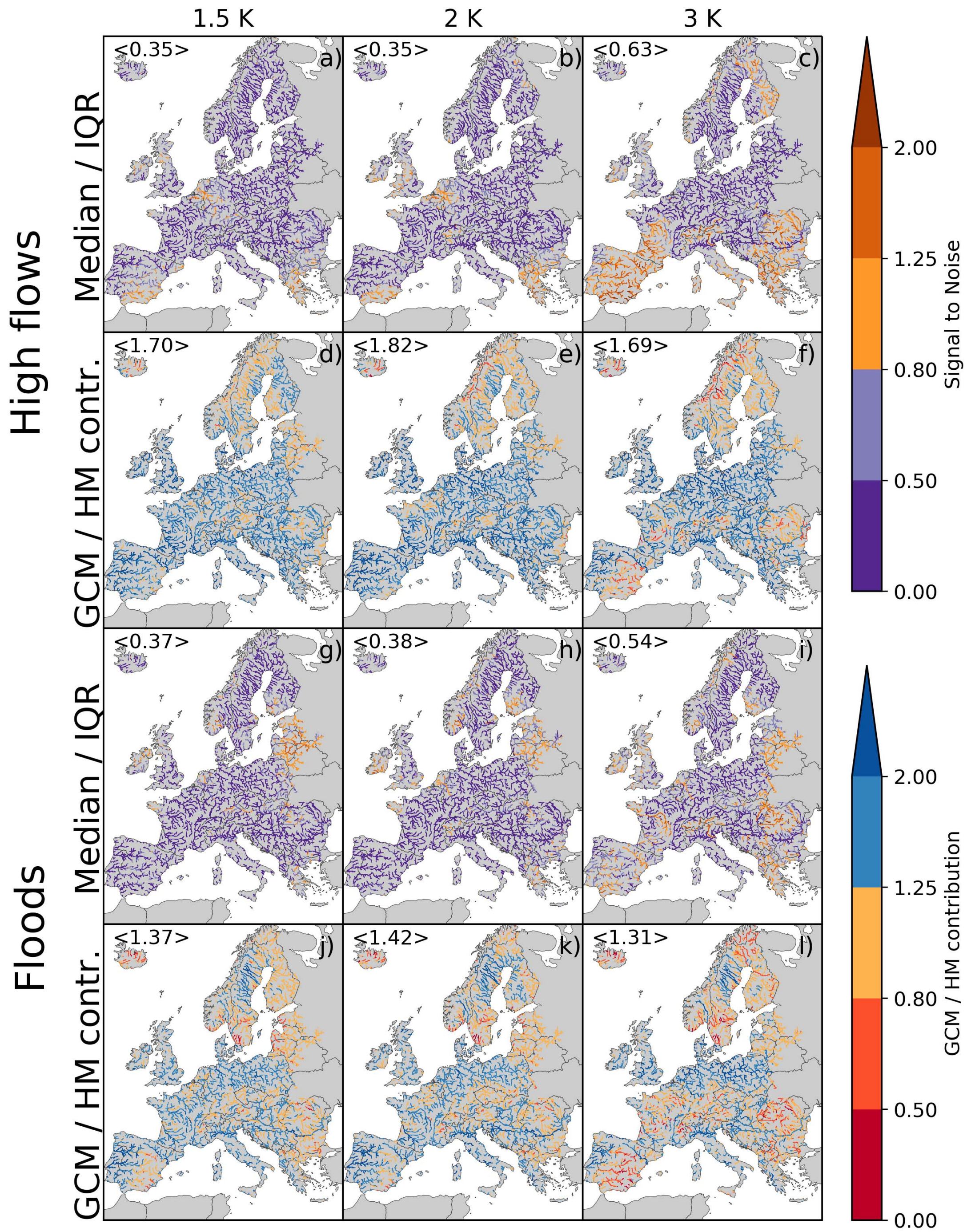

Figure 4. Signal to noise ratio calculated as ratio between multi-model ensemble median and ensemble inter-quartile range (IQR) is depicted for high flow indicator (panels (*a*)–(*c*)) and floods (panels (*g*)–(*i*)). The ratio between the GCM contribution and HM contribution to the uncertainty (IQR) is shown for high flows (panels (*d*)–(*f*))and floods (panels (*j*)–(*l*)). The levels for GCM/HM contribution are symmetric around 1 for a multiplicative measure. The numbers given in $< \cdot >$ denote the spatial average.

(figure 3). These results should not be confused with the fact that a 2 K warming from the 1980s in comparison to 1.5 K from the 1980s shows more substantial changes. The temperature difference in both cases is larger than 0.5 K and the variability of the dataset is too large to identify significant differences given a 0.5 K warming. Adaptation is required for both 1.5 and 2 K warming, but adaptation actions could be similar for both warming levels. These include water resources management, flood protection, and the design of infrastructures.

3.3. Uncertainty contribution by general circulation models and hydrologic models

The signal to noise ratio (SNR), expressed as the ensemble median divided by the ensemble inter-quartile range (Giuntoli *et al* 2015), is small for changes in floods and high flows under all warming levels in Europe. SNR is less than one in about 70% of the rivers under investigation (figure 4). This implies that there is a substantial uncertainty in the multi-model median presented in figure 1 and it is challenging to derive quantitatively-based adaptation from these results. SNR is on average higher for high flows than for floods (compare figures 4(*a*)–(*c*) and figures 4(*g*)–(*i*)). This indicates that floods exhibit a higher ensemble variability than high flows. Lower signal to noise ratios are generally found for 1.5 K warming level in comparison to 2 K and 3 K warming because the magnitude of relative changes also increases with increased warming (figure 1) and thus strengthens the signal. The spatial patterns of SNR follow those of the relative changes with hotspots of strong decreasing signals in the Mediterranean for high flows and the Baltic countries for increasing floods. Overall, these results highlight that there is substantial uncertainty associated with the results presented in this study. There is a mixed pattern regarding the uncertainty contribution of GCMs and HMs on changes in high flows (figures 4(*d*)–(*f*)) and floods (figures 4(*j*)–(*l*)). Overall, in 75% of Europe, uncertainty is dominated by GCMs (relative GCM/HM uncertainty contribution > 1.25) for the high flow indicator irrespective of the warming level. For floods, the relative GCM contribution is significantly lower, dominating around 50% of the area under 1.5 K and 2 K global warming and about 40% for 3 K global warming. This implies that the choice of HM substantially contributes to the uncertainty of the results in 25% up to 60% of the area. A higher spread induced by HMs has also been found in Donnelly *et al* (2017), although no rigorous uncertainty contribution was conducted in that study. The results of this study also confirm the findings of Dankers *et al* (2014) who stated that the use of a single hydrologic model underestimates the uncertainty in projected floods in their global scale analysis. It can be expected that GCMs are the main contributor to the high flow uncertainty because this indicator has shown a large dependency on precipitation changes (figure 2). Such a relationship could not be found for the flood indicator, which depends, among others, more strongly on antecedent wetness condition (Bloeschl *et al* 2013). Hotspots of HM uncertainty are areas with a high contribution of snowmelt to runoff or in semi-arid regions (e.g. Scandinavia, the Iberian Peninsula, and the Balkans). Under dry conditions, the representation of soil moisture dynamics and runoff processes has a large impact on the simulation results. For instance, the fraction of fast surface runoff is relatively higher for Noah-MP than for mHM and PCR-GLOBWB because it does not use linear reservoirs to delay the runoff signal. In regions with a considerable snow cover, different representations of snow processes enhance the variability caused by HMs. Noah-MP solves the full energy balance of snow, whereas mHM and PCR-GLOBWB use a degree-day factor approach. High uncertainty contribution in snow-dominated regions was also reported by Giuntoli *et al* (2015).

The 45 ensemble members used in this study consider only two major sources of uncertainty (i.e. choice of GCM and HM). This underestimates the true uncertainty of projected changes because of two reasons. First, the used GCMs and HMs only cover a fraction of the possible projections by all GCM/HM combinations (McSweeney and Jones 2016). Second, other factors influencing the uncertainty do exist. These include the choice of downscaling technique, bias-correction method, choice of reference period, internal climate variability, hydrologic model parameters and model resolution (Wilby 2005, Deser *et al* 2014, Kundzewicz *et al* 2017). For example, other downscaling techniques such as dynamical and statistical downscaling schemes will provide different representation of extreme precipitation and altered climate change signals (Jacob *et al* 2014, Donnelly *et al* 2017, Themeßl *et al* 2012). These should be recognised in future studies.

4. Summary and conclusions

The magnitude of climate change has diverse impacts on European river high flows (10% exceedance probability of streamflow) and floods (annual maximum). Decreases are projected for both high flows (up to −31%) and floods (up to −17%) in the Mediterranean and Eastern Europe mostly related to decreases in total annual precipitation. In Northern regions, high flows are projected to increase due to increasing precipitation, but floods are projected to decrease due to less snowmelt. In these regions, adaptation to climate change thus has to be designed explicitly for the metric in mind, which has to be chosen according to stakeholder requirements.

Changes in river floods are sensitive, non-linearly, to global warming. The magnitude and robustness of results are generally increasing with increased global warming levels. A detailed investigation of the differences between present-day (1980s) and a 1.5, 2, and 3 K warmer world revealed that significant changes occur between the 1980s and 1.5 K global warming and changes to 3 K global warming. The effort to limit global warming to 1.5 K (UNFCC 2015) might result in smaller changes compared to 2 K global warming, but these could not be identified as robust given the variability of the underlying data. In summary, adaptation measures have to be taken regardless of this 0.5 K change in global warming. Adaptation could be similar under 1.5 K and 2 K global warming, but have to account for significantly higher changes under 3 K global warming.

The signal to noise ratio, which is used to estimate uncertainty in projected changes, increases with increasing warming level. Both GCMs and HMs contribute to the uncertainty. The share by HMs is substantial in semi-arid regions such as the Iberian Peninsula and the Balkans and regions with a considerable snow season (e.g. Scandinavia). This highlights the fundamental requirement of considering multiple HMs and that impact assessments only using a single HM might be misleading. Only two sources of uncertainty, the choice of GCM and HM, were considered in this study. Future studies should account for additional uncertainties origination from internal climate variability and choice of downscaling method. A further avenue for research is improving the process representation and accuracy of HMs in those regions where they dominate the uncertainty in the projections (i.e. snow-dominated and semi-arid locations). Even with the limited analysis considered in this study, uncertainties are too high to derive quantitatively-based adaptation measures over larger parts of Europe.

Acknowledgments

This study has been mainly funded within the scope of the HOKLIM project (www.ufz.de/hoklim) by the German Ministry for Education and Research (grant number 01LS1611A). This study has been partially funded by the Copernicus Climate Change Service. The European Centre for Medium Range Weather Forecasts implements this service and the Copernicus Atmosphere Monitoring Service on behalf of the European Commission. We would like to thank all the colleagues who contributed to the EDgE project (http://edge.climate.copernicus.eu/). We acknowledge the funding from NWO Rubicon 825.15.003. The ENSEMBLES data used in this work was funded by the EU FP6 integrated project Ensembles (contract number 505539) whose support is gratefully acknowledged. We acknowledge the E-OBS dataset from the EU FP6 project ENSEMBLES (http://ensembles-eu.metoffice.com) and the data providers in the ECA&D project (http://www.ecad.eu). We are also grateful to the ISIMIP project for providing the climate model data for this study. This ISIMIP project was funded by the German Federal Ministry of Education and Research (BMBF) with project funding reference number 01LS1201A. We would like to thank people from various organizations and projects for kindly providing us the data which were used in this study, which includes JRC, ESA, NASA, USGS, GRDC, BGR & UNESCO, ISRIC, EEA, EWA, and CEDEX.

ORCID iDs

Stephan Thober https://orcid.org/0000-0003-3939-1523
Niko Wanders https://orcid.org/0000-0002-7102-5454

References

Alfieri L, Burek P, Feyen L and Forzieri G 2015 Global warming increases the frequency of river floods in Europe *Hydrol. Earth Syst. Sci.* **19** 2247–60

Andréasson J, Bergström S and Carlsson B 2004 Hydrological change–climate change impact simulations for Sweden *AMBIO J. Human Environ.* **33** 228–34

Arheimer B and Lindstrom G 2015 Climate impact on floods: changes in high flows in Sweden in the past and the future 1911–2100 *Hydrol. Earth Syst. Sci.* **19** 771–84

Bierkens M F P *et al* 2015 Hyper-resolution global hydrological modelling: what is next? Everywhere and locally relevant *Hydrol. Process.* **29** 310–20

Bloeschl G *et al* 2017 Changing climate shifts timing of European floods *Science* **357** 588–90

Bloeschl G, Nester T, Komma J, Parajka J and Perdigao R A P 2013 The June 2013 flood in the upper Danube basin, and comparisons with the 2002, 1954 and 1899 floods *Hydrol. Earth Syst. Sci.* **17** 5197–212

Blum A G, Archfield S A and Vogel R M 2017 On the probability distribution of daily streamflow in the United States *Hydrol. Earth Syst. Sci.* **21** 3093–103

Bosshard T, Kotlarski S, Zappa M and Schär C 2014 Hydrological climate-impact projections for the Rhine river: GCM-RCM uncertainty and separate temperature and precipitation effects *J. Hydrometeorol.* **15** 697–713

Chow V T, Maidment D R and Mays L W 1988 *Applied Hydrology* (New York: Tata McGraw-Hill Education)

Collins M *et al* 2013 Long-term climate change: projections, commitments and irreversibility *Climate Change 2013: The Physical Science Basis. Contribution of Working Group I to the Fifth Assessment Report of the Intergovernmental Panel on Climate Change* ed T F Stocker *et al* (Cambridge: Cambridge University Press)

Cuntz M, Mai J, Samaniego L, Clark M, Wulfmeyer V, Branch O, Attinger S and Thober S 2016 The impact of standard and hard-coded parameters on the hydrologic fluxes in the Noah-MP land surface model *J. Geophys. Res.: Atmos.* **121** 10676–700

Dankers R *et al* 2014 First look at changes in flood hazard in the Inter-sectoral Impact Model Intercomparison Project ensemble *Proc. Natl Acad. Sci.* **111** 3257–61

Deser C, Phillips A S, Alexander M A and Smoliak B V 2014 Projecting North American climate over the next 50 years: uncertainty due to internal variability *J. Clim.* **27** 2271–96

Donnelly C, Greuell W, Andersson J, Gerten D, Pisacane G, Roudier P and Ludwig F 2017 Impacts of climate change on European hydrology at 1.5, 2 and 3 degrees mean global warming above preindustrial level *Clim. Change* **143** 13–26

Giuntoli I, Vidal J P, Prudhomme C and Hannah D M 2015 Future hydrological extremes: the uncertainty from multiple global climate and global hydrological models *Earth Syst. Dyn.* **6** 267–85

Gosling S N *et al* 2016 A comparison of changes in river runoff from multiple global and catchment-scale hydrological models under global warming scenarios of 1 °C, 2 °C and 3 °C *Clim. Change* **141** 577–95

Guha-Sapir D, Below R and Hoyois P 2017 EM-DAT: The Emergency Events Database (www.emdat.be)

Hall J *et al* 2014 Understanding flood regime changes in Europe: a state-of-the-art assessment *Hydrol. Earth Sys. Sci.* **18** 2735–72

Hattermann F F, Huang S, Burghoff O, Hoffmann P and Kundzewicz Z W 2016 Brief communication: an update of the article modelling flood damages under climate change conditions—a case study for Germany *Nat. Hazards Earth Syst. Sci.* **16** 1617–22

Hawkins E *et al* 2017 Estimating changes in global temperature since the preindustrial period *Bull. Am. Meteorol. Soc.* **98** 1841–56

Haylock M R, Hofstra N, Klein Tank A M G, Klok E J, Jones P D and New M 2008 A European daily high-resolution gridded data set of surface temperature and precipitation for 1950–2006 *J. Geophys. Res.: Atmos. 1984–2012* **113** D20119

Hempel S, Frieler K, Warszawski L and Schewe J 2013a Bias corrected GCM input data for ISIMIP Fast Track *GFZ Data Services* (www.isimip.org/gettingstarted/fast-track-bias-correction/) (Accessed: 8 December 2017)

Hempel S, Frieler K, Warszawski L, Schewe J and Piontek F 2013b A trend-preserving bias correction—the ISI-MIP approach *Earth Syst. Dyn.* **4** 219–36

Jacob D *et al* 2014 EURO-CORDEX: new high-resolution climate change projections for European impact research *Reg. Environ. Change* **14** 563–78

James R, Washington R, Schleussner C-F, Rogelj J and Conway D 2017 Characterizing half-a-degree difference: a review of methods for identifying regional climate responses to global warming targets *Wiley Interdiscip. Rev. Clim. Change* **8** e457

Kay A L and Jones D A 2012 Transient changes in flood frequency and timing in Britain under potential projections of climate change *Int. J. Climatol.* **32** 489–502

Kovats R S, Valentini R, Bouwer E, Georgopulou E, Jacob D, Martin E, Rounsevell M and Soussana J-F 2014 Europe *Climate Change 2014: Impacts, Adaptation, and Vulnerability. Part B: Regional Aspects. Contribution of Working Group 2 to the Fifth Assessment Report of the Intergovernmental Panel on Climate Change* ed V R Barros *et al* (Cambridge: Cambridge University Press) pp 1267–1326

Krysanova V and Hattermann F F 2017 Intercomparison of climate change impacts in 12 large river basins: overview of methods and summary of results *Clim. Change* **141** 363–79

Kumar R, Samaniego L and Attinger S 2013 Implications of distributed hydrologic model parameterization on water fluxes at multiple scales and locations *Water Resour. Res.* **49** 360–79

Kundzewicz Z W *et al* 2017 Differences in flood hazard projections in Europe—their causes and consequences for decision making *Hydrol. Sci. J.* **62** 1–14

McSweeney C F and Jones R G 2016 How representative is the spread of climate projections from the 5 CMIP5 GCMs used in ISI-MIP? *Clim. Serv.* **1** 24–9

Mendoza P A, Clark M P, Mizukami N, Newman A J, Barlage M, Gutmann E D, Rasmussen R M, Rajagopalan B, Brekke L D and Arnold J R 2015 Effects of hydrologic model choice and calibration on the portrayal of climate change impacts *J. Hydrometeorol.* **16** 762–80

Metzger M J, Bunce R G H, Jongman R H G, Mücher C A and Watkins J W 2005 A climatic stratification of the environment of Europe *Glob. Ecol. Biogeogr.* **14** 549–63

Niu G-Y *et al* 2011 The community Noah land surface model with multiparameterization options (Noah-MP): 1. Model description and evaluation with local-scale measurements *J. Geophys. Res.* **116** D12109

Rajczak J, Pall P and Schär C 2013 Projections of extreme precipitation events in regional climate simulations for Europe and the Alpine Region *J. Geophys. Res.: Atmos.* **118** 3610–26

Rakovec O, Kumar R, Mai J, Cuntz M, Thober S, Zink M, Attinger S, Schäfer D, Schrön M and Samaniego L 2016 Multiscale and multivariate evaluation of water fluxes and states over European river basins *J. Hydrometeorol.* **17** 287–307

Rojas R, Feyen L, Bianchi A and Dosio A 2012 Assessment of future flood hazard in Europe using a large ensemble of bias-corrected regional climate simulations *J. Geophys. Res.: Atmos.* **117** D17109

Roudier P, Andersson J C M, Donnelly C, Feyen L, Greuell W and Ludwig F 2016 Projections of future floods and hydrological droughts in Europe under a +2 °C global warming *Clim. Change* **135** 341–55

Samaniego L, Kumar R and Attinger S 2010 Multiscale parameter regionalization of a grid-based hydrologic model at the mesoscale *Water Resour. Res.* **46** W05523

Samaniego L *et al* 2017 Propagation of forcing and model uncertainties on to hydrological drought characteristics in a multi-model century-long experiment in large river basins *Clim. Change* **141** 435–49

Themeßl M J, Gobiet A and Heinrich G 2012 Empirical-statistical downscaling and error correction of regional climate models and its impact on the climate change signal *Clim. Change* **112** 449–68

UNFCC 2015 Adoption of the Paris agreement, Proposal by the President *Technical report* (Geneva: United Nations) (http://unfccc.int/resource/docs/2015/cop21/eng/l09r01.pdf)

van Beek L P H, Wada Y and Bierkens M F P 2011 Global monthly water stress: 1. Water balance and water availability *Water Resour. Res.* **47** W07517

van Vliet M T H, Donnelly C, Strömbäck L, Capell R and Ludwig F 2015 European scale climate information services for water use sectors *J Hydrol.* **528** 503–13

Vautard R *et al* 2014 The European climate under a 2 °C global warming *Environ. Res. Lett.* **9** 034006

Vogel R M and Fennessey N M 1994 Flow-duration curves I: new interpretation and confidence intervals *J. Water Res. Plan. Manage.* **120** 485–504

Wanders N and Wada Y 2015 Human and climate impacts on the 21st century hydrological drought *J Hydrol.* **526** 208–20

Warszawski L, Frieler K, Huber V, Piontek F, Serdeczny O and Schewe J 2014 The Inter-sectoral Impact Model Intercomparison Project: project framework *Proc. Natl Acad. Sci.* **111** 3228–32

Wasko C and Sharma A 2017 Global assessment of flood and storm extremes with increased temperatures *Sci. Rep.* 7–7945

Wilby R L 2005 Uncertainty in water resource model parameters used for climate change impact assessment *Hydrol. Process.* **19** 3201–19

Wood E F *et al* 2011 Hyperresolution global land surface modeling: meeting a grand challenge for monitoring Earth's terrestrial water *Water Resour. Res.* **47** W05301